MINISTRY OF EDUCATION AND TRAINING

VIETNAM ACADEMY OF SCIENCE AND TECHNOLOGY

GRADUATE UNIVERSITY OF SCIENCE AND TECHNOLOGY

NGUYEN MINH TUAN

STUDY ON THE FABRICATION OF LINER FOR SHAPED CHARGE DEVICES USING ULTRA-FINE GRAIN COPPER AND W-Cu COMPOSITES

SUMMARY OF DISSERTATION ON METALLOLOGY

Code: 9.44.01.29

Hanoi - 2024

The dissertation is completed at: Graduate University of Science and Technology, Vietnam Academy Science and Technology

Supervisors:

1. Supervisor 1: Assoc. Prof. Dr. Đoan Đinh Phuong
2. Supervisor 2: Assoc. Prof. Nguyen Van Tich

Reviewer 1: .....

Reviewer 2: .....

Reviewer 3: .....

The dissertation will be examined by Examination Board of Graduate University of Science and Technology, Vietnam Academy of Science and Technology at…….. (time, date……)

The dissertation can be found at:

1. Graduate University of Science and Technology Library
2. National Library of Vietnam

INTRODUCTION

1. The necessary of the thesis

A shaped charge is an explosive charge that is designed to concentrate the explosive energy by deforming a liner in the concave surface of the explosive block. This results in the creation of a high-speed metal jet in a solid state, which can penetrate various materials such as steel armor, concrete, and rock…. used in various industrial sectors, including oil and gas exploration, transportation, mining, and military. In the military, the shaped charge principle with a metal liner is applied to prepare different anti-armor bullets ranging in size from 30 to 150 mm such as artillery shells, grenade launchers, controllable anti-tank missiles, cluster munition elements for air force bombs and multiple-firing rocket artillery shells. The shaped charge effect is also used in weapons for large-sized combats such as anti-ship cruise missiles, torpedoes, anti-submarine mines at high depths, and mines dropped in sea and rivers.

In Vietnam, the Ministry of National Defense has carried out numerous programs and activities to develop, test, and produce anti-tank ammunition. Many products have been integrated into Army weapons, including B41M, PG-9, and 40 mm shaped charge bullets... However, in the fabrication process, there are still some limitations. The penetration is unstable and not equal to similar foreign products. Through analysis, the main reason is still in the prepared liners. Therefore, the research topic: ***"Study on the fabrication of liner for shaped charge devices using ultra-fine grain copper and W-Cu composites"*** was selected to focus on the fabricating of the liner with greater penetration ability for military applications.

2. The goals of the thesis

- Fabrication and characterization of microstructure, properties of ultra-fine grain copper and W-Cu composites.
- Fabrication of liners using ultra-fine grain copper and W-Cu composite and evaluating the penetration properties of liners made by the above two materials.

3. The main research content of the thesis

- Study on preparing copper liner by 4 different processing methods: (i) cold stamping, (ii) cold stamping followed up spinning, (iii) sintered by SPS, and (iv) sintered by SPS followed up spinning. Investigating the properties, and structures and then evaluating and comparing the penetration ability of 4 types of prepared liners through explosion testing.
- Study on preparing W-Cu composite liners by SPS sintering and SPS sintering and then spinning. Investigating the properties, and structures and then evaluating and comparing the penetration ability of two types of prepared liners through explosion testing.

The novel contributions of the thesis

- A fabrication process has been developed and successfully implemented for making shaped charge liners using ultrafine-grained copper and ultrafine-grained matrix W-Cu composites via the powder metallurgy method. This process utilizes spark plasma sintering techniques followed by mechanical spinning.
- The penetration characteristics of the fabricated shaped charge liners were studied using both simulation methods and experimental explosion tests. The optimal composition of the W-Cu composite was found to be 50% Cu and 50% W, resulting in a penetration depth increase of approximately 10% compared to a pure copper liner.

Chapter 1. OVERVIEW

- Presents the history, structure and principles of shaped charge devices.

- Presents some factors that affect the performance of shaped charge devices such as cone shape, number of explosives, the structure of shaped charge device, focal length and detailed machining tolerances during the assembly process.

- Overview of some types of materials used for preparing liners. Up to now, many different materials have been tested for applications in the liner. Copper and its alloys are among the most commonly used materials according to the principles of density and plastic deformability. Besides the influence of the kind of materials, other factors such as grain size on penetration depth are also discussed in detail. The structure of the metal cone material has an important influence on the performance of liners. With the same material, the smaller the particle size, the higher the efficiency of liners.

- The techniques employed in fabricating metal liners include stamping and rolling using metal and their alloys. Nevertheless, the powder metallurgy technique offers distinct benefits in the production of metal composite liners including metal constituents with different melting temperatures and densities. Currently, many advanced sintering processes including microwave sintering, hot pressing, and spark plasma sintering (SPS), are used to enhance the density of liners.

- The applications of shaped charge devices are summarized as in light weapons, detonators, bombs, mines, grenades, and especially in artillery shells and rockets. …

Chapter 2. RESEARCH METHODS

2.1. Materials

2.1.1. Copper sheet

A copper sheet (C10100) with a purity of 99.97 % and thickness of 1.5 mm, was used to fabricate liner by two different methods including cold stamping and cold stamping combined with spinning.

2.1.2. Copper powder

Copper powder synthesized by electrolysis with a dendritic shape has a purity of 99.5% and a particle size in the range of 44–74 µm.

2.1.3. Tungsten powder (W)

The W powder with an angular shape has a purity of 99.9% and an average particle size of 50 µm.

2.1.4. Other chemicals

- Gases: H_2 with a purity of 99,99% was used for the reduction process and Ar with a purity of 99.99 % for cleaning.

- Other materials and chemicals used in the process of fabricating and cleaning samples include Alcohol, acetone, n-hexane, paraffin...

2.2. Fabrication methods

2.2.1. Bulk samples

Samples were fabricated by powder metallurgy method, including 100% copper and W-Cu composite samples. The samples were prepared according to successive stages: milling, pressing, shaping, preliminary sintering, and SPS.

2.2.2. Liner samples

The W-Cu composite liners are prepared by powder metallurgy, using the SPS technique. Liners made of Cu are made by both methods including cold stamping and powder metallurgy.

2.3. Characterization methods

2.3.1. Microstructure

2.3.1.1. Optical microscopy (OM) and scanning electron microscopy (SEM)

To study the structure of the cone material, the sample is taken from the center position of the liner by wire cutting method. Then the sample was ground, impregnated with $FeCl_3$ solution (5g) + HCl (10mL) + H_2O (100mL). The microstructure of the materials was studied using optical microscopes (Axiovert 40 MAT, Germany), scanning electron microscope (SEM, Hitachi S4800, Japan), and transmission electron microscope HR-TEM (JEOL JEM) 2100, Japan).

2.3.1.2. Transmittance electron microscopy (TEM)

The sample was cut from the liners with a diameter of ϕ 3 mm and a thickness of 0.5 mm using a wire-cutting device. The sample after thinning is preliminarily examined on optical glass. After that, the sample continues to be electrochemically etched in H_3PO_4 solution (Electrolite D2) on a TenuPol-5 device (Struers, USA) to ensure that the electron beam can penetrate the sample.

2.3.2. Methods for mechanical properties

2.3.2.1. Density

The density of the samples was measured by the Archimedes method on the AND GR-202, Japan, located at the Institute of Materials Science-VAST.

2.3.2.2. Hardness

A microhardness tester (IndentaMet 1106, Buehler United States) was used to determine the microhardness of the samples.

2.3.3. Penetration ability test

2.3.3.1. Simulation study using ANSYS AUTODYN software

- Introduction of ANSYS AUTODYN software
- Simulation process

Step 1: Create a file to save data and choose the simulation model.

Step 2: Building the material models and parameters.

Step 3: Boundary selection

Step 4: Building geometric models (choosing element types, mesh types, building geometric models...) This work is carried out directly in the working environment of Ansys AutoDyn -2D.

Step 5: Setting initial conditions and interaction conditions.

Step 6: Running, collecting results and analyzing.

2.3.3.2. Shaped charge testing

The explosive device consists of a steel body, a W-Cu liner and 38±1 grams of H11 explosive as shown in Figure 2.16. Steel target made of 40Cr steel (C = 0.38-0.44%, Cr = 0.8-1.1%) has a diameter of 80 mm and a thickness of 120 mm.

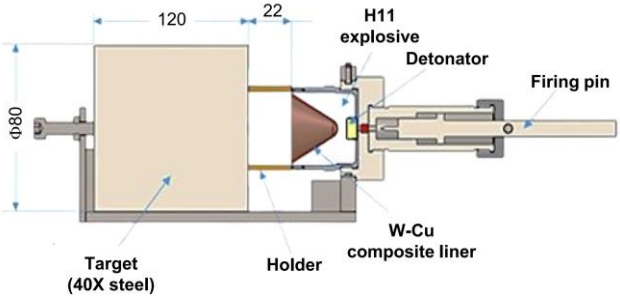

Figure 2.16. The schematic of the test system for the shaped charge.

Chapter 3. FABRICATION, STRUCTURE AND SHAPED CHARGE PROPERTIES OF ULTRA-FINE GRAIN COPPER

3.1. Fabrication of ultra-fine-grained metal liners

Two methods were used to fabricate the metal liners: (i) Fabrication of metal liner from copper sheet by cold stamping technique; (ii) Fabrication of metal liner from copper powder by SPS. The overview process for the fabrication of liner by two methods is presented in Figure 3.1.

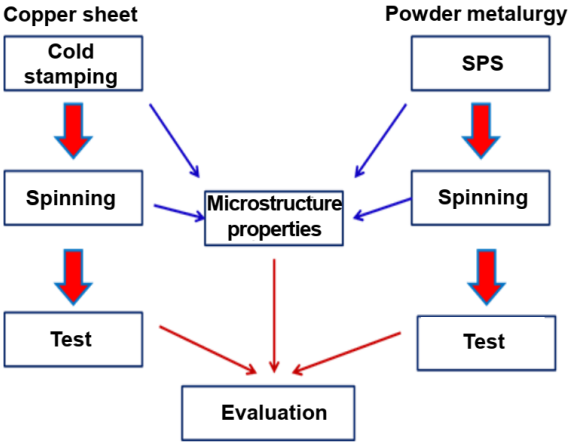

Figure 3.1. Fabrication process of liners using two methods

3.1.1. Fabrication of liner by cold stamping

The process of the liner from a copper sheet by cold stamping method has been described in Section 2.2.2 of Chapter 2.

3.1.2. Fabrication of liner using SPS

Liners were fabricated by powder metallurgy method using the SPS technique described in Section 2.2.2, Chapter 2.

3.1.3. Fabrication of liner by using spinning technique after cold stamping and SPS

To obtain copper liners with an ultra-fine grain structure, the liners after cold stamping or after sintering with SPS were continued to the machining process as described in Section 2.2.2 of Chapter 2.

3.2. Structure and properties of liners fabricated by cold stamping and SPS

3.2.1. Structure and properties of liners fabricated by cold stamping

3.2.1.1. Structure of cold stamped liners

In Figure 3.8, As observed the OM image of the structure of liners prepared by the cold stamping liner and the cold stamping combined with the spinning after etching. The structure consists of polycrystalline particles with sizes from a few tens to hundreds of μm, multi-sided shapes with different sizes (Figure 3.8a). However, as can be seen in Figure 3.8b, the grains tend to grow in certain dimensions and decrease in the other dimension.

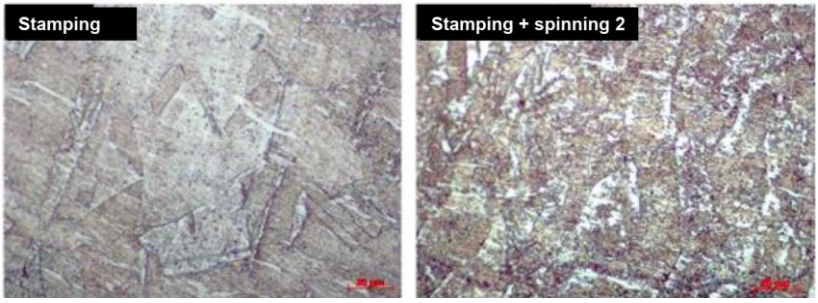

Figure 3.8. OM images of liners fabricated by (a) cold stamping and (b) cold stamping combined with spinning.

3.2.1.2. Mechanical and physical properties of cold stamped liners

The measured hardness and density of the liners prepared by using the stamping and spinning deformation are presented in Figure 3.10. The obtained results showed that, with the stamping technique, the hardness of the sample is 114.3 HV. After the first time spinning,

the hardness of the samples increases to 116.6 HV and then reaches a value of 119.4 HV for the sample processed with the second spinning. Meanwhile, the density of the samples is the same.

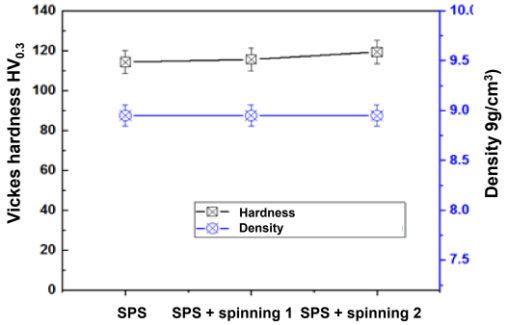

Figure 3.10. The dependence of hardness and density of liners prepared by stamping and after spinning deformation.

3.2.2. Structure and properties of liners fabricated by SPS

3.2.2.1. Structure of liners fabricated by SPS

The OM images of liners prepared by SPS and a combination of SPS and spinning are shown in Figure 3.11. The structure of the sample fabricated by SPS is also polycrystalline. As for the SPS sintered copper sample combined with spinning, the OM image showed that the structure consists of flat and long particles.

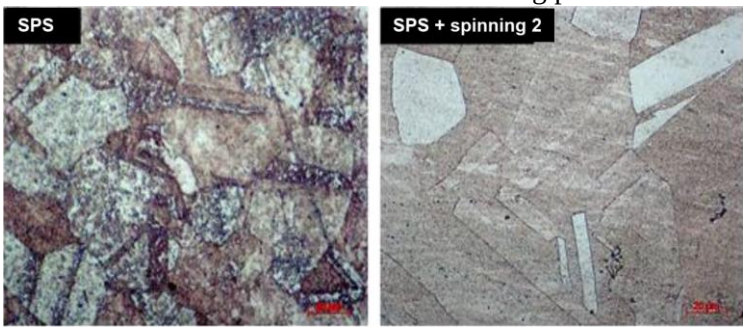

Figure 3.11. OM image of liners prepared by (a) SPS technique and SPS combined with spinning technique

3.2.2.2. Mechanical and physical properties of SPSed liners

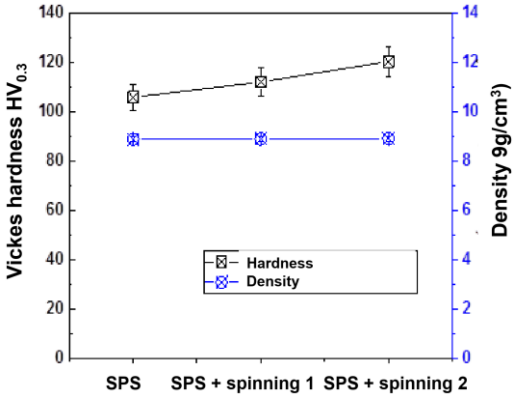

Figure 3.13. The dependence of hardness and density of liners prepared by SPS and after spinning deformation.

Figure 3.13 shows the results of measured hardness and density of SPSed liners and after the first and second spinning process. The Vickers hardness increases after spinning deformation.

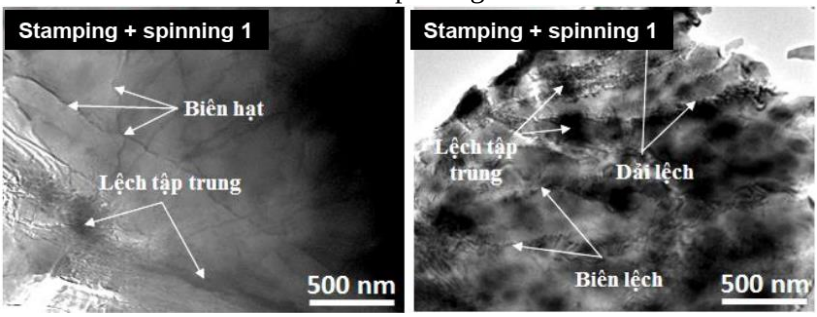

Figure 3.12. TEM images of the cold stamped liner after (a) the first spinning and (b) the second spinning.

The results of TEM analysis of the liner prepared by cold stamping after the first and second time of spinning are presented in Figure 3.12. For the liners after the first spinning, the presence of dislocations was absorbed, but the grain boundaries were still seen

(Figure 3.12a). When continuing to deform with the second spinning, many dislocations walls appeared with a higher concentration of dislocations (Figure 3.12 b). In other words, the dislocation density after the second spinning is increased.

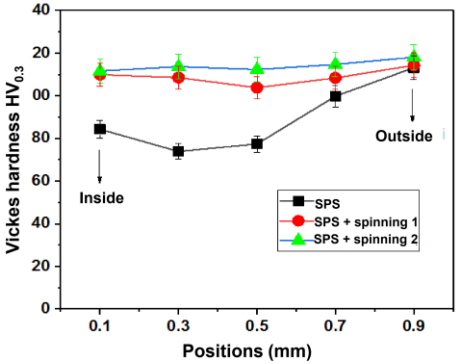

Figure 3.13. Microhardness of stamped liners after spinning deformation at different positions.

Figure 3.13 shows that the microhardness of the stamped liners has a large difference at the measured positions. At the measured positions near the inner and outer surfaces, the hardness values are higher than the center position. this may be because there have been certain dislocations of the surface of the liners on both sides of the liners.

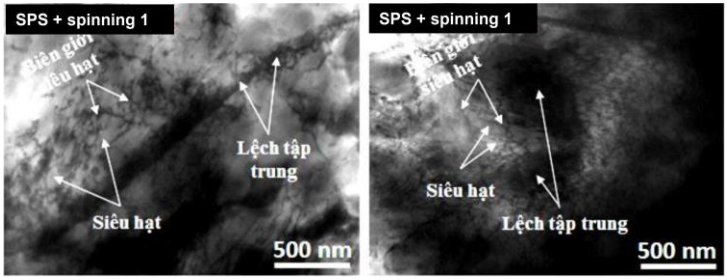

Figure 3.14. TEM image of SPSed liner after (a) first spinning and (b) second spinning

The results of TEM images of the SPSed liners after the first spinning and after the second spinning are given in Figure 3.14. Observations on the SPSed liners combined with the first spinning (Figure 3.14a) showed the presence of boundaries along with ultra-fined grains with sizes ranging from several tens to several hundred nm. When the liner sample continues to be deformed for the second time, boundaries and ultra-fined grains with smaller sizes than the first deforming sample are formed and many areas with the presence of concentrated dislocations (Figure 3.14 b).

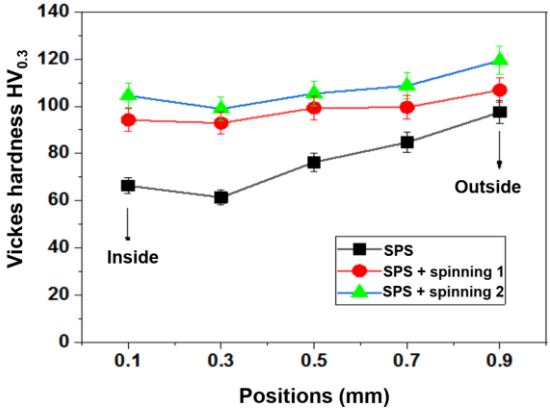

Figure 3.15. Microhardness of SPSed liners after spinning deformation at different positions.

3.3. Shaped charge testing results of fabricated liners

From Table 3.1, it can be seen that the penetration depth of the liner prepared by the cold stamping method is the lowest and most unstable, varying over 20%. The highest penetration depth was obtained with liners prepared by the SPS and then combined with the spinning deformation.

Table 3.1. The value of measured penetration depth of different liners.

No	Type of samples	Penetration depth (first test) (mm)	Penetration depth (second test) (mm)	Average Penetration depth (mm)
1	Liners prepared by cold stamping	45	55	**50**
2	Liners prepared by cold stamping + spinning	80	81	**80,5**
3	Liners prepared by SPS	71	70	**70,5**
4	Liners prepared by SPS + spinning	82	80	**81**

Chapter 4: FABRICATION, STRUCTURE AND SHAPED CHARGE PROPERTIES OF ULTRA-FINE GRAIN W-Cu COMPOSITE

4.1. Study the effect of W content on the penetration ability of liners using simulation software

The penetration depth (P) of the shaped charge will depend on the jet length formed after the explosive reaction occurs and the density of the liner according to formula (1.3):

$$P \sim L(\lambda.\rho_j/\rho_t)^{1/2} \quad (1.3)$$

Where L is the jet length, ρ_j is the density of the liner, ρ_t is the density of the target material, and λ is the coefficient related to the jet length with a value in the range from 1 to 2.

Table 4.2. Composition and theoretical density of the W-Cu composites with different W contents

Samples	Cu contents (wt.%)	W contents (wt.%)	Theoretical density (g/cm^3)
Cu	100	0	8.96
Cu70W30	70	30	10.67
Cu60W40	60	40	11.40
Cu50W50	50	50	12.23
Cu40W60	40	60	13.19

Using A-IX-1 with a composition (93.5-95)% RDX and (4-6.5)% tamed, As for the Cu liner, the simulation results show that the υ_1 achieved before hitting the target was determined at about 6357 m/s with, the L of 43mm and the P of 80mm as showed in Figure 4.2.

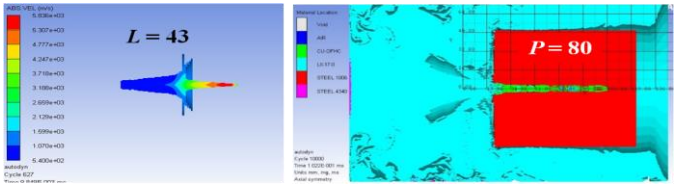

Figure 4.2. Simulation result of Cu liners

Figure 4.3 shows the jet velocity of the W-Cu composite liner with different W contents. The obtained results indicated that the jet velocity of W-Cu composite liners was decreased with the increase of W content. With Cu70W30 composite, the jet velocity was calculated to be 6288 m/s. When increasing the W content up to 60%, the jet velocity is only 5446 m/s which is decreased by 14.3% compared to pure Cu liner.

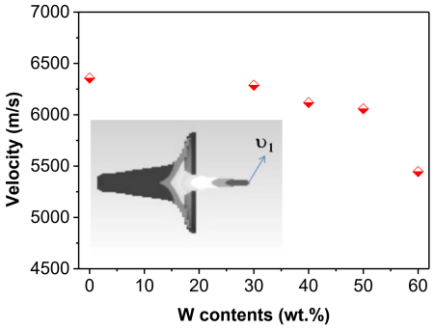

Figure 4.3. The jet velocity of W-Cu composite liner with different W contents

Figure 4.8 shows the dependence of metal jet length L, penetration depth P and theoretically calculated density on W content. With W content increasing from 0 to 60%, the density of the

composite sample increases. up because W has a higher density than Cu (its density is 2.15 times higher than Cu). When continuing to increase the W content to 60 %, the penetration depth P rapidly decreases to 85 mm (10.5 % reduction compared to 50% W content), even lower when compared to cones with W content is 40%.

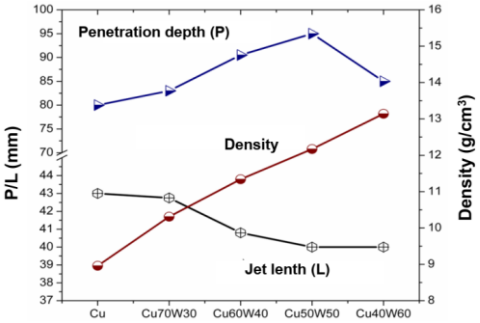

Figure 4.8. The dependence of the jet length, the penetration depth and the density of the W-Cu composite liners on W content

4.2. Fabrication and actual testing of W-Cu composite liners

4.2.1. Effect of W content on structure and properties of W-Cu composite liners

Figure 4.10 shows the SEM images of W-Cu composite liners containing different W contents after SPS sintering. W particles (white) were fairly uniformly dispersed within the Cu matrix (gray).

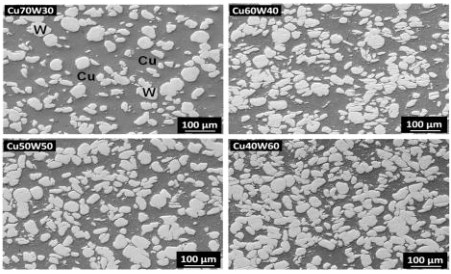

Figure 4.10. SEM images liners with different W contents (a) Cu70W30, (b) Cu60W40, (c) Cu50W50 and (d) Cu60W40.

the density of the W- Cu composites increased with increasing W content, from 8.89 to 12.76 g/cm3 corresponding to W content from 0 to 60 wt.%. Compared to the theoretically calculated density, the measured density is lower.

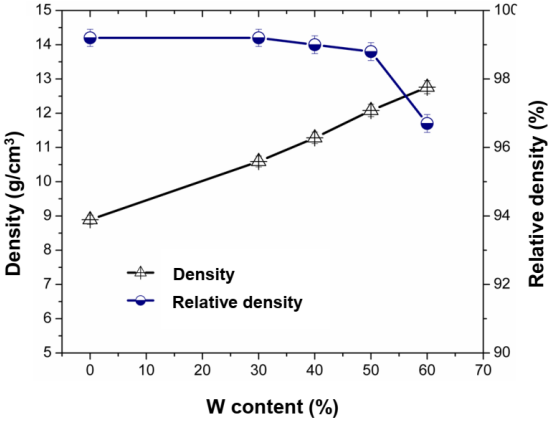

Figure 4.15. Density and relative density of W-Cu composite liners containing different W contents.

When increasing the W content, the hardness of the W-Cu composite increases rapidly, the hardness reached 126.3 HV for the composite contained 30 wt.% W and reached the highest value of 209.2 HV for the composite reinforced by 60 wt.% W.

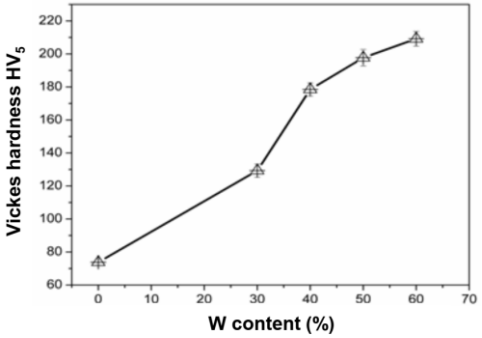

Figure 4. 16. Vickers hardness of liners with different W contents.

4.2.2. Shaped charge testing results of W-Cu composite liners

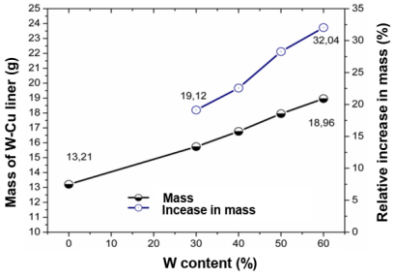

Figure 4.17. Effect of W content on the mass of W-Cu liners and their relative mass increase.

Figure 4.17 shows that the weight of the liners prepared by copper powder after SPS reached 13.21g and then increased to 18.96g with a W content of 60% by weight.

The prepared W-Cu composite liners were introduced to the shape charge test. The tests were carried out under the same test conditions including the same explosive type, explosive mass and 40Cr steel target to compare the penetration depth of the prepared composite liners. Figure 10 shows the OM of the cross-section along the penetration depth on a 40Cr steel target after testing.

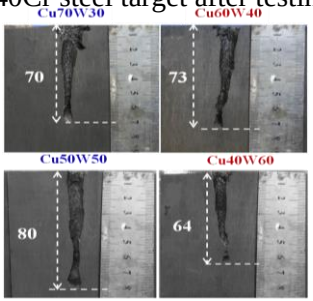

Figure 4.18. Cross section along the penetration depth on a 40Cr steel target after testing of (a) Cu70W30, (b) Cu60W40, (c) Cu50W50 and (d) Cu60W40.

4.3. Spinning machining for ultra-fine grain structure

4.3.1. Microstructure of Cu50W50 composite liners after SPS

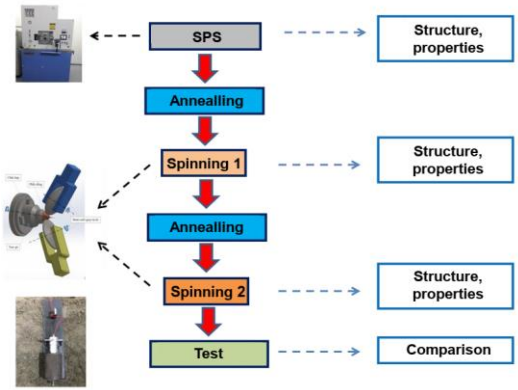

Figure 4.20. The fabrication process of ultra-fine-grained Cu50W50 composite liner

SEM images and optical images of the Cu50W50 sample after SPS are shown in Figure 4.23. The structure of Cu contains many grains several tens to hundreds of mm in size in the form of alternating sheets and the boundaries between polycrystalline Cu grains can still be observed.

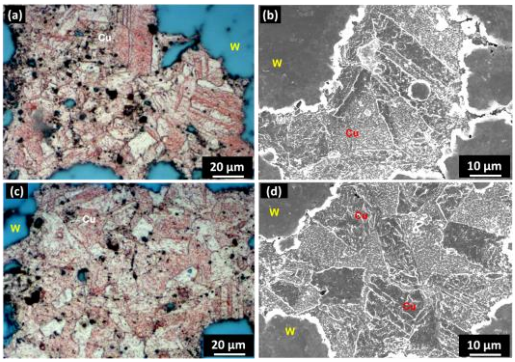

Figure 4.23. OM and SEM images of Cu50W50 composite liners after SPS.

4.3.2 Microstructure of Cu50W50 composite liners after spinning 1

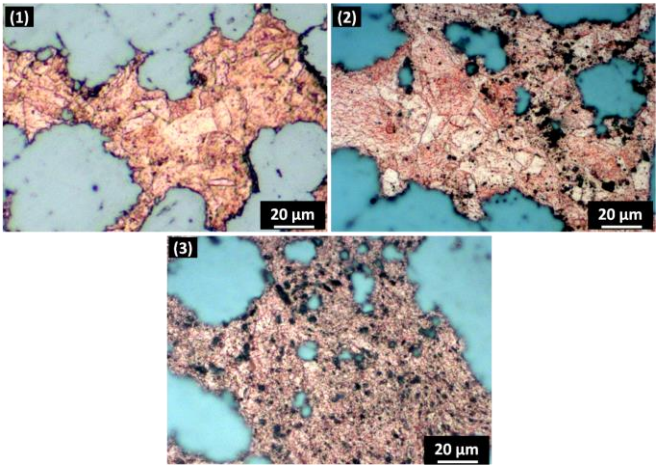

Figure 4.24. Optical images of W-Cu composite liner after spinning 1 at different positions (1) inside, (2) center and (3) outside.

Figure 4.24 is the optical images of the liner wall after spinning, polishing and etching. Positions 1, 2, and 3 correspond to the structure of the section going from the inner surface to the outer surface of the liner wall (the position in contact with the roller of the spinning device).

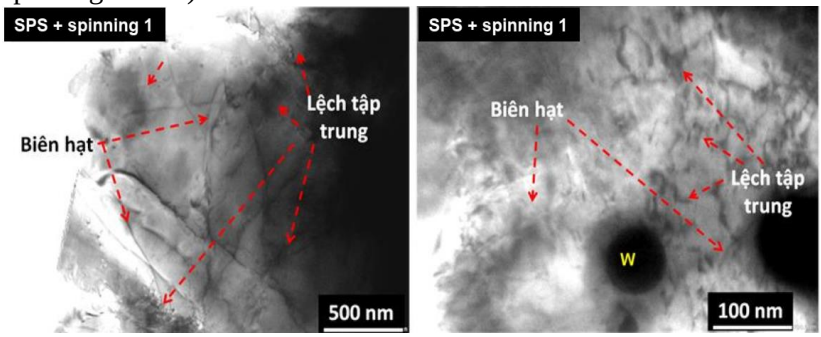

Figure 4.26. TEM images of microstructure of outside of liner wall after spinning 1.

The structure of the outer surface of the liner wall is observed and shown in Figure 4.26. The obtained results indicated that ultra-fine grains with a maximum size of a few hundred nm.

4.3.3 Microstructure of Cu50W50 composite liners after spinning 2

Figure 4.27 shows optical images of the cross-sectional surface of the liner wall with corresponding positions from the inside to the outside of the cone wall similar to the sample after the first spinning. Observation on the optical image of the Cu-rich positions shows that It can be seen that, there are no longer any coarse Cu grains from the inner to the outer wall of the cone.

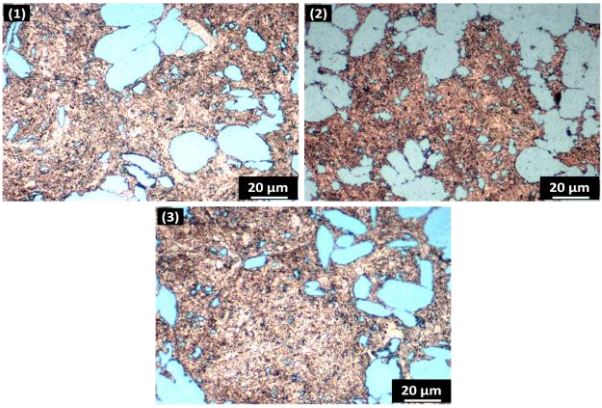

Figure 4.27. Optical images of W-Cu composite after spinning 2.

The structure of the ultra-fine Cu grains after the second spinning was also observed on TEM as shown in Figure 4.29. From the TEM image, the dispersed formation of dislocations in the supergrain is observed. In addition, a stronger and more concentrated formation of dislocations leading to the formation of the dislocation walls at the boundaries is also observed.

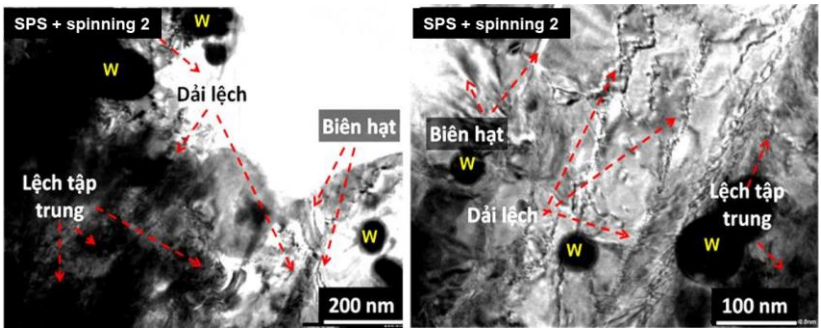

Figure 4.29. TEM image of the outside liner after spinning 2

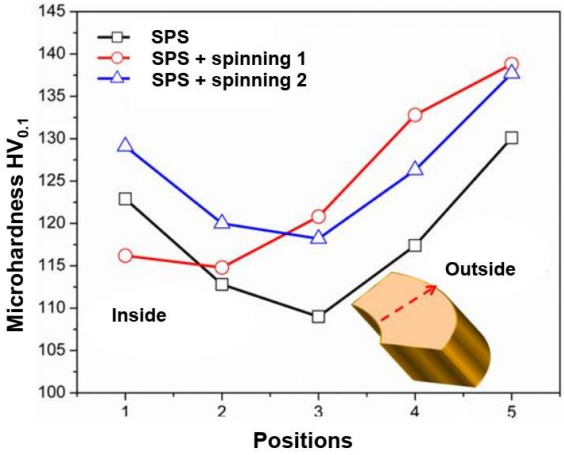

Figure 4.31. Microhardness of Cu50W50 composite liner after SPS, 1st and 2nd spinning.

The results of determining the Vickers hardness HV0.1 of the copper-rich region of the Cu50W50 composite liner after SPS, after the first spinning and after the second spinning are shown in the graph of Figure 4.31. The general trend observed is that the hardness on the outer wall will be higher than that of the inner wall. This is different from the obtained results of Cu liner prepared by cold stamping and cold stamping combined with spinning, SPS sintering, or SPS sintering combined with spinning.

4.3.4 Shaped charge test of W-Cu composite liners after spinning 2

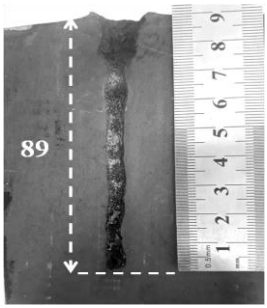

Figure 4.34. Cross section along the penetration depth on a 40Cr steel target after testing.

The obtained results show that the penetration depth of W-Cu composite liners has increased significantly after spinning 2. The average measured penetration depth is about 89 mm on a 40X steel target as shown in figure 4.34.

Figure 4.36 summarizes the penetration depth of Cu and Cu50W50 liners fabricated by cold stamping, SPS sintering and combined machining. The results indicated the role of the ultra-fine grain structure in both Cu and Cu50W50 liners.

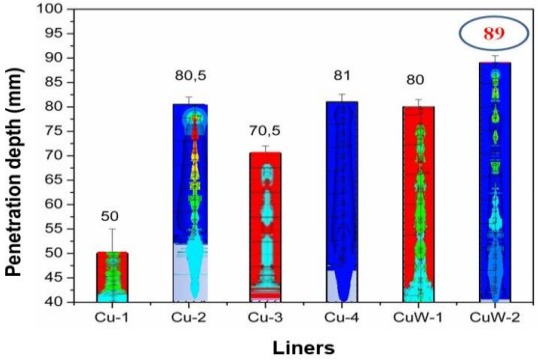

Figure 4.36. Comparison on penetration depth of: Cu-1: stamping, Cu-2: Stamping + spinning, Cu-3: SPS, Cu-4: SPS + spinning, CuW-1: Cu50W50 SPS và CuW-2: - Cu50W50 SPS + spinning 2

CONCLUSION

The thesis has focused on studying the fabrication method of shaped charge liners, the structure, properties and penetration ability of two types of liners with ultra-fine structures including Cu and W-Cu composite. Based on the obtained results, some main conclusions can be drawn as follows:

Cu shaped charge liners:

1. Successfully prepared liners for shaped charge devices by powder metallurgy methods from copper powder using the SPS technique. The prepared samples exhibited a polycrystalline structure, with grain sizes ranging from 50 to 200 μm. Liners prepared by SPS penetrate steel 41% deeper than that of liners prepared by using the conventional cold stamping technique.

2. Ultra-fine-grained structure of liners was successfully prepared by employing the spinning technique. The structure of the liner after spinning consists of polycrystalline grains, inside these grains are sub-grains with sizes ranging from 300-500 nm. The penetration depth of the Cu liner after spinning increases by 15% compared to the penetration of liners prepared by the SPS and increases by 60% compared to the liner prepared by the cold stamping technique.

W-Cu composite-shaped charge liners:

3. By using simulation and experimental, the optimized composition of W/Cu composite was determined to be 50% W and 50% Cu to fabricate a liner with a maximum penetration depth.

4. Successfully fabricated W-Cu composite liner using 50%W+50%Cu using powder metallurgy method with SPS technique.

5. The grain size of the Cu matrix in the 50W50Cu composite strongly affects the penetration depth of the liners. The 50W50Cu composite liners prepared by SPS, have an ultra-fine structure, including grains with sizes from 100-300 nm. The penetration depth of the 50W50Cu liner after spinning increased by 11% compared to the liner prepared by SPS, without the spinning process.

6. Grain size (super grain) and dislocation density of the liners influence the penetration depth of the shaped charge devices. Small grain size and high dislocation density could help the deformation of liner according to the principle of superplasticity, and thus increase the continuity of the jet, thereby increasing the penetration depth.

NEW CONTRIBUTIONS OF THE THESIS

- A technological process has been built to successfully fabricate the liner for shaped charge devices by using the powder metallurgy method. The ultra-fine-grained Cu and W-Cu composite could be prepared by using the combination of spark plasma sintering and spinning techniques.

- The penetration characteristics of the fabricated shaped charge liners were studied using both simulation methods and experimental explosion tests. The optimal composition of the W-Cu composite was found to be 50% Cu and 50% W, resulting in a penetration depth increase of approximately 10% compared to a pure copper liner.

LIST OF THE PUBLICATIONS RELATED TO THE DISSERTATION

[1]. **Nguyễn Minh Tuấn**, Trần Bảo Trung, Đoàn Đình Phương, Lương Văn Đương, Nguyễn Ngọc Linh, Nguyễn Văn Toàn *"Nghiên cứu ảnh hưởng của một số phương pháp chế tạo phễu lót đến chiều sâu xuyên thép của lượng nổ lõm",* Tạp chí nghiên cứu KH&CN Quân sự; Số 85, 2-2023; pp. 142-151; ISSN: 1859 – 1043.

[2]. **Nguyen Minh Tuan**, Nguyen Ngoc Linh, Nguyen Van Toan *"Effect of Heating Rate and Sintering Temperature on Mechanical Properties of W-Cu Composites Produced via Spark Plasma Sintering",* International Journal of Engineering Research & Science (IJOER); Vol-8, Issue-10, October- 2022; pp. 1-6; ISSN: 2395-6992.

[3]. **Nguyen Minh Tuan,** Nguyen Van Toan, Luong Van Duong, Vu Thang Long, Tran Bao Trung, Pham Van Trinh, Doan Dinh Phuong *"Microstructure and microhardness of conical shaped W-Cu composites prepared by spark plasma sintering and subsequent spinning process"*; *IEEE Access* (accepted for publication); DOI 10.1109/ACCESS.2024.3351759 (SCIE, IF = 3,9)

[4]. **Nguyen Minh Tuan,** Nguyen Van Toan, Vu Thang Long, Luong Van Duong, Pham Van Trinh, Tran Bao Trung, Doan Dinh Phuong *"Effect of Tungsten Contents on the Jet Penetration Performance of Shaped Charge Liner Based Copper-Tungsten Composites"*; *Frontiers in Materials*; Volume 11 – 2024, doi: 10.3389/fmats.2024.1308290 (SCIE, IF = 3,2)